



**HAL**  
open science

## A double focusing SAXS camera with $\mu\text{m}$ focal spot based on a circular bragg-fresnel lens

A. Snigirev, I. Snigireva, C. Riekkel, A. J. Miller, L. Wess, T. Wess

### ► To cite this version:

A. Snigirev, I. Snigireva, C. Riekkel, A. J. Miller, L. Wess, et al.. A double focusing SAXS camera with  $\mu\text{m}$  focal spot based on a circular bragg-fresnel lens. *Journal de Physique IV Proceedings*, 1993, 03 (C8), pp.C8-443-C8-446. 10.1051/jp4:1993891 . jpa-00252322

**HAL Id: jpa-00252322**

**<https://hal.science/jpa-00252322>**

Submitted on 4 Feb 2008

**HAL** is a multi-disciplinary open access archive for the deposit and dissemination of scientific research documents, whether they are published or not. The documents may come from teaching and research institutions in France or abroad, or from public or private research centers.

L'archive ouverte pluridisciplinaire **HAL**, est destinée au dépôt et à la diffusion de documents scientifiques de niveau recherche, publiés ou non, émanant des établissements d'enseignement et de recherche français ou étrangers, des laboratoires publics ou privés.

## A double focusing SAXS camera with $\mu\text{m}$ focal spot based on a circular Bragg-fresnel lens

A. SNIGIREV, I. SNIGIREVA, C. RIEKEL\*, A. MILLER\*\*, L. WESS\*\* and T. WESS\*\*

*Institute of Microelectronics Technology, Russian Academy of Sciences, 142 432 Chernogolovka, Moscow Region, Russia*

*\* ESRF, BP. 220, 38043 Grenoble cedex, France*

*\*\* Department of Biochemistry, University of Edinburgh, Medical School, Edinburgh, EH8 9XD, U.K.*

A 2D focusing SAXS camera has been build based on a circular Bragg-Fresnel lens. The camera has been tested at the Microfocus beamline at the European Synchrotron Radiation Facility. An undulator was used as radiation source. The focused beam size at the sample position of about  $1.5 \times 2 \mu\text{m}^2$  and intensity of about  $10^9$  photons/s was obtained at a wavelength of  $1.24 \text{ \AA}$  (10keV). A Molecular Dynamics image plate was used to detect the low -angle diffraction pattern. For native turkey leg tendon collagen intermediate areas between the calcified and non-calcified regions were analysed. More than 22 orders including the first order peak were clearly resolved.

### Introduction

X-ray small angle scattering is a well established standard technique for diffraction studies of a wide range of naturally occurring and synthetic materials. However the need for high angular resolution in SAXS technique made it difficult to develop high spatial resolution cameras because of considerable loss of flux due to collimation of the beam. The combination of microfocusing X-ray optics - based on a Bragg-Fresnel lens (BFL)- being developed for hard X-ray applications [1-4] with the high brilliance X-ray beams provided by third generation synchrotron radiation sources open up new opportunities to design SAXS cameras for measuring diffraction patterns from samples in specific regions of micron dimensions. This technique can be applied to a range of biological materials. For example, analysis of the intermediate area between the calcified and non-calcified sections of turkey leg tendon required micrometer size beam since this area is very small ( $200\text{-}500 \mu\text{m}$ )[5].

### Experiment

The performance of the BFL-based SAXS camera has been tested at the Microfocus beamline at the ESRF. The experimental setup is shown in Fig.1. A low- $\beta$  undulator with the source size  $\sigma_x \times \sigma_z = 150 \times 90 \mu\text{m}^2$  was located at a distance of 36m from the camera. The 10keV monochromatic beam was selected by a Si channel-cut nitrogen-cooled monochromator [6] and was focused on a sample by a circular Bragg-Fresnel lens using the 555-reflection in nearly backscattering geometry [2,4]. The BFL has been fabricated on the (111) surface of the silicon single crystal and the basic parameters of the BFL are: innermost zone width  $2r_1 = 17.5 \mu\text{m}$ ; outermost zone width  $\Delta r_n = 0.4 \mu\text{m}$ ; aperture,  $A = 200 \mu\text{m}$ . The focal distance of the lens was  $F = 0.62 \text{ m}$ . The demagnification factor was therefore about 60, which gives a focal spot at the sample of about  $2 \mu\text{m}$  in diameter. In Fig.2 one can see an image of the focused beam on high resolution Kodak film placed a few millimetres behind the focal plane (sample position). The central high intensity focal spot is surrounded by the geometric shadow of the BFL aperture region, where the intensity

is reduced substantially because only a small fraction of the incident beam is delivered to the zero diffraction order for phase BFL[4]. The intensity beyond the BFL shadow is due to reflection by the flat Si crystal outside of the BFL area. This reflection can be easily cut by the horizontal and vertical slits installed downstream of the lens just before the specimen. The width of the slits should be slightly smaller than the BFL aperture.

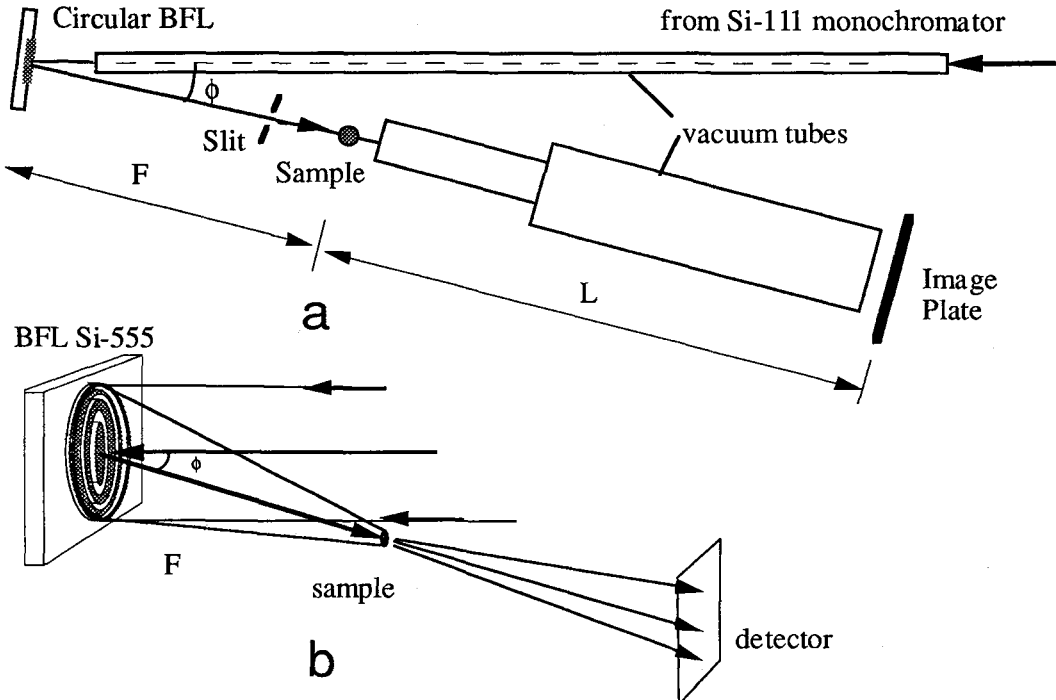


Fig.1 (a) Schematic layout (top view) of the BFL-based SAXS camera: deviation from normal incidence:  $\phi=6^\circ$ ; focal distance:  $F=0.62\text{m}$ ; distance sample-to-detector:  $L=1.3\text{m}$ . (b) Schematic figure of the optical principle of X-ray focusing by a circular BFL in backscattering geometry.

The angular resolution of our SAXS camera is defined by the divergence of the beam at the sample and is equal to the ratio of the BFL aperture to the focal distance:  $A/F=3\cdot 10^{-4}$  radian, that means the samples with the spacings less than  $3000\text{\AA} - 4000\text{\AA}$  can be studied using the proposed camera.

It is useful to make a comparison of the BFL-based camera with a pinhole-based camera without focusing element. One can easily show that the intensity is greater in the case of focusing optics by factor  $\epsilon(A/\delta)^2$ , where  $\epsilon$  is the diffraction efficiency of the lens, and  $\delta$  is the focal spot diameter. In our case the BFL of  $200\mu\text{m}$  diameter and 25% efficiency for 10 keV gives  $2.5\cdot 10^3$  more photons in  $2\mu\text{m}$  spot than does a  $2\mu\text{m}$  pinhole. This value also gives us the signal-to-noise ratio. Taking into account the loss of intensity due to backscattering geometry by factor 10, the flux density in the spot is more than 100 times higher compared with the pinhole collimation and equals  $\sim 10^7$  ph/s/ $\mu\text{m}^2/\text{mA}$ .

The sample stage consists of a three-axis manual-driven translation stage ( $x,y,z$ ) at the base, X-axis stepping motor-driven translation stage in the centre and a standard Huber goniometer head with two axis of

rotation at the top. The (x,y,z) stage is used for preliminary adjustment of the collagen of 200-400  $\mu\text{m}$  thickness in the  $\mu\text{m}$  focus beam. The X stage is used for scanning the collagen during the analysis.

Locating the sample in the  $\mu\text{m}$  X-ray beam was done as follows. First, using the (xyz) stage the tip of a needle was placed instead of the sample on the goniometer head and adjusted in the focused beam. An "X-ray eye" camera was used for preliminary alignment. Final alignment was done using high resolution film. An x-ray image of the tip near the focal spot is shown in fig.2(a). Second, the needle was replaced by the sample and the centre of the sample roughly corresponded to the tip of the needle. Using the (x,y,z) stage the point of the sample to be studied was moved into the beam (Fig.2b,c). This point can be set in the X-ray focused beam to within a few microns. Finally, the microfocus beam was selected by slits of 50-100 $\mu\text{m}$  width (schematically shown with dashed lines in Fig.2c).

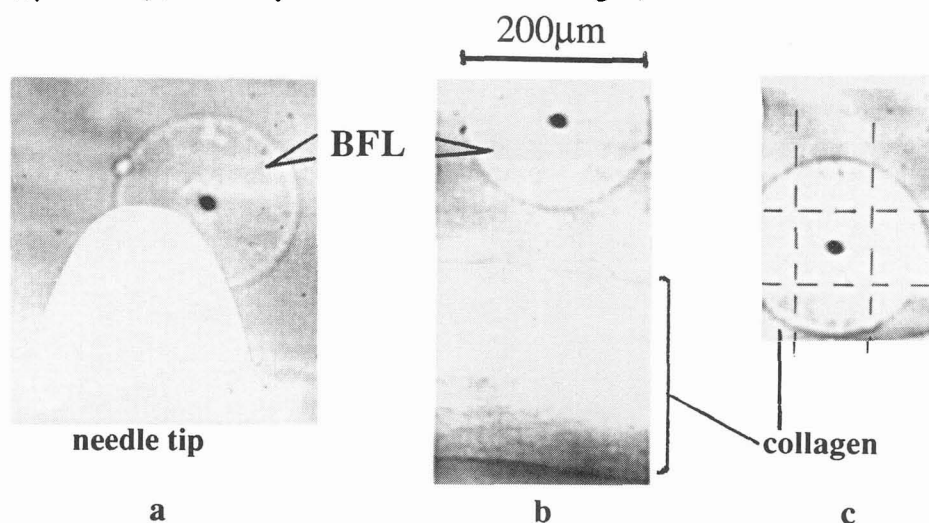


Fig.2 X-ray images for the different steps of the adjustment of the sample in the  $\mu\text{m}$ -beam.

The X-rays diffracted from the sample were detected on the Molecular Dynamics image plate (IP) of 250mm length and 200mm width. The distance between the IP and the sample was about 1.3m. The exposure time was about 10-15min. The read out pixel size is  $176 \times 176 \mu\text{m}^2$  and dynamic range for luminescence detection is from 0 to  $10^5$ .

The diffraction patterns from the different areas of turkey leg tendon collagen are shown in fig.3. The first 22 meridional reflections were resolved. It was observed that reflections from calcified collagen have much higher intensity than those from non-calcified area of tendon. Detailed analysis will be done in future publication. One can easily see the resolution potential of the camera. Very sharp diffraction peaks of about  $300 \mu\text{m}$  width and 3mm distance are observed. This implies that 5-8 times larger Bragg spacings than collagen ( $670 \text{\AA}$ ) can be resolved by the camera discussed above.

### Conclusion.

The present results show for the first time that small-angle scattering is possible from a sample on the scale of a few  $\mu\text{m}$  and can possibly be extended to the sub $\mu\text{m}$  range in future. This opens the possibility for new applications of SAXS, in particular in the area of surfaces and interfaces. The important feature of

proposed camera is the fact that one can measure down to the smallest angles without using a complicated collimation system: defining and guard apertures (slits).

One of the another attractive feature of the optical setup is a well defined shape of the focused beam and that the intensity distribution in the focus spot has a high degree of azimuthal symmetry. This is very desirable for SAXS measurements if the accurate form of the scattering curve is required.

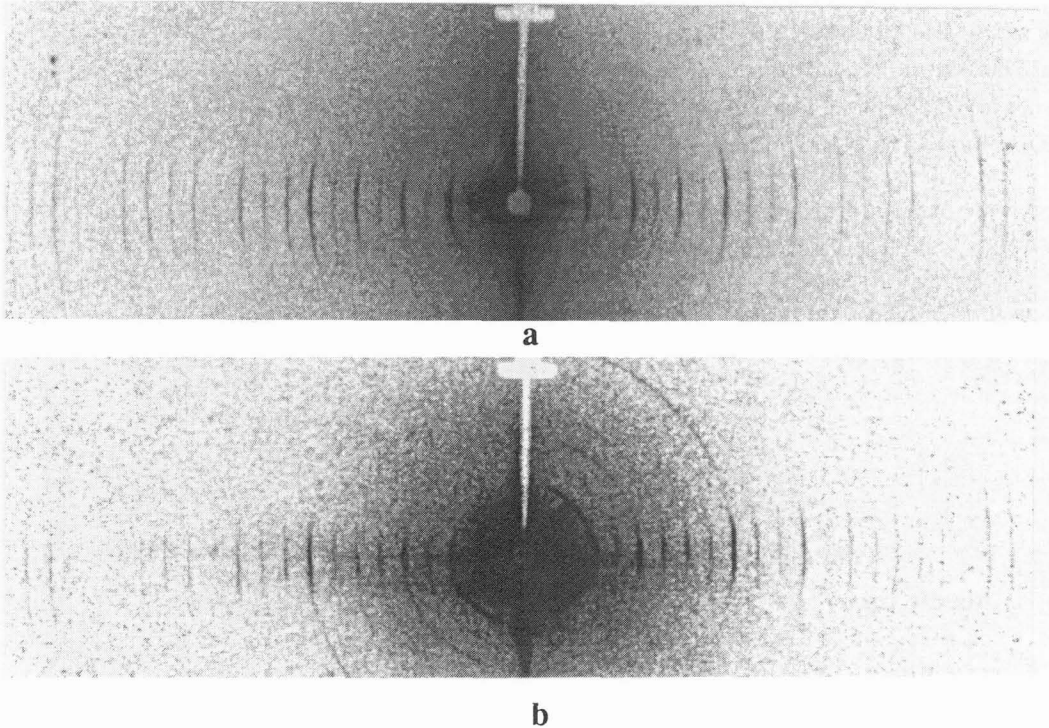


Fig.3 Low-angle x-ray diffraction patterns of the turkey leg tendon collagen obtained in BFL-based SAXS camera using Molecular Dynamics image plate:  
a - non-calcified area; b -calcified area

### Acknowledgment

The authors acknowledge the support of the ESRF Elastic Diffuse Scattering Group, especially M.Kocsis, P.Bösecke, O.Diat, P.Wattecamps. We gratefully acknowledge the support of the Alexander-von-Humboldt Foundation (A.A.Snigirev).

### References

- [1] Aristov V.V., Snigirev A.A., Basov Yu.A., Nikulin A.Yu., AIP Conf. Proc.147 (1986) 253.
- [2] Basov Yu.A., Pravdivtseva T.L., Snigirev A.A., Belakhovsky M., Dhez P., Freund A., Nucl. Instrum.&Methods A308 (1991) 363.
- [3] Bonse U., Riekel C., Snigirev A.A., Rev. Sci. Instrum. 63 (1992) 622.
- [4] Snigirev A., Snigireva I., Chavanne J., Elleaume P., Hartman Ya., Tarazona E., Rev. Sci. Instrum. (1993) to be published
- [5] White S.W., Hulmes D.J.S., Miller A., Timmins P.A., Nature 266 (1977) 421.
- [6] Bösecke P., Holmberg J., ESRF Newsletters, 17 (1993) 10.